CLOSE-RANGE PHOTOGRAMMETRY WITH VIDEO CAMERAS

A. W. Burner, W. L. Snow, W. K. Goad
NASA Langley Research Center
Hampton, VA 23665

ABSTRACT

Examples of photogrammetric measurements made with video cameras uncorrected for electronic and optical lens distortions are presented. The measurement and correction of electronic distortions of video cameras using both bilinear and polynomial interpolation are discussed. Examples showing the relative stability of electronic distortions over long periods of time are presented. Having corrected for electronic distortion, the data are further corrected for lens distortion using the plumb line method. Examples of close-range photogrammetric data taken with video cameras corrected for both electronic and optical lens distortion are presented.

INTRODUCTION

The use of film cameras for photogrammetry may not be practical in a hostile inaccessible environment. In such cases an alternative is to use video cameras for the desired photogrammetric measurements. At NASA Langley Research Center the National Transonic Facility (NTF) is a large wind tunnel capable of high pressure (up to 9 atm), low temperature (below 100 K) operation (Howell 1980). Cameras located within the tunnel pressure plenum will be used to measure the deflection of aircraft model wings under aerodynamic load. Brooks and Beamish (1977) performed similar experiments in a conventional transonic wind tunnel. Since the cameras at the NTF will be inaccessible for long periods of time, video cameras were selected for the initial photogrammetric measurement (Burner, Snow, and Goad 1983).

A number of papers have been devoted to the use of video cameras for space applications (Wong 1970, 1973, 1975) and their potential for close-range photogrammetry, especially in hazardous environments has been recognized. The nature and stability of electronic distortions present in video images were of concern in early investigations. It was found that the geometrical distortions of video cameras were largely systematic and relatively stable over long periods of time so that corrections were possible, especially if a calibrated reseau grid was located on the photoconductive surface of the video tube. It was also noted that a large portion of the geometrical distortion was caused by scale differences between the horizontal and vertical axes of the video image. Simple scale corrections could remove large amounts of video distortion. Of several approaches for correcting the residual electronic distortion of video images, two techniques emerged for close-range applications--bilinear interpolation and high-order polynomial interpolation. High-order polynomial interpolation was favored by Wong and has more recently been applied to video images measured with an electronically generated cursor (Sieffert 1982). The use of a faceplate reseau grid allows the independent treatment of electronic distortion. Further data refinement to account for optical distortion is necessary for best results.

The video camera delivers the image data to a suitable hardcopy device. The permanent records can be measured and interpreted using conventional photogrammetric methods. This paper experimentally examines the assumed fidelity of this transfer process and the data refinement required to utilize standard photogrammetric models for interpretation. The improved metric stability of solid state cameras and the potential advantage of automated data readup using image processing techniques, while recognized, are not treated in this paper.

PHOTOGRAMMETRIC MEASUREMENTS WITHOUT DISTORTION CORRECTIONS

Although for optimum results the video images should be corrected for both electronic and optical lens distortion, photogrammetry with video cameras uncorrected for distortion (except for scale differences between the horizontal and vertical axes) is worthy of discussion. Such measurements would be useful for inexpensive video cameras which do not have reseau grids on the photoconductive surface of the tube and for preliminary results using video tubes which do have reseau grids.

The video cameras used for this study were instrumentation grade, high resolution (up to 1200 TV lines) cameras which were operated at 875 raster scan lines with 2:1 interlace. Two types of high resolution (600-900 TV lines of resolution at center of tube) video tubes have been used--the Vidicon and Newvicon. The more sensitive Newvicon tubes are currently being used at NTF to allow operation at higher lens F-numbers with consequent greater depth of field. Standard television lenses of 50 mm focal length are used.

Since the objective of this study was to prepare for measurements at the NTF, the close-range photogrammetric measurements presented duplicate the camera locations and pointing angles at the NTF. The camera locations at the NTF were dictated by viewing port locations and mounting constraints. The experimental configuration consists of two video cameras separated by 0.91 meter. The optical axes of the cameras converge to the center of the aircraft model wing under test (Figure 1). The bisector of the base between the two cameras is 2 meters from the center of the wing. The angle of convergence between the two cameras is approximately 25°. Recordings of the video images are made with a video hardcopy unit which records video images on dry silver paper in a 17 x 23 cm format. The hard copy unit takes 4 seconds to record a video image and the image is available for viewing after 11 seconds. In order to read the dry silver hardcopies on the monocomparator, the hardcopies must be illuminated from above. A high

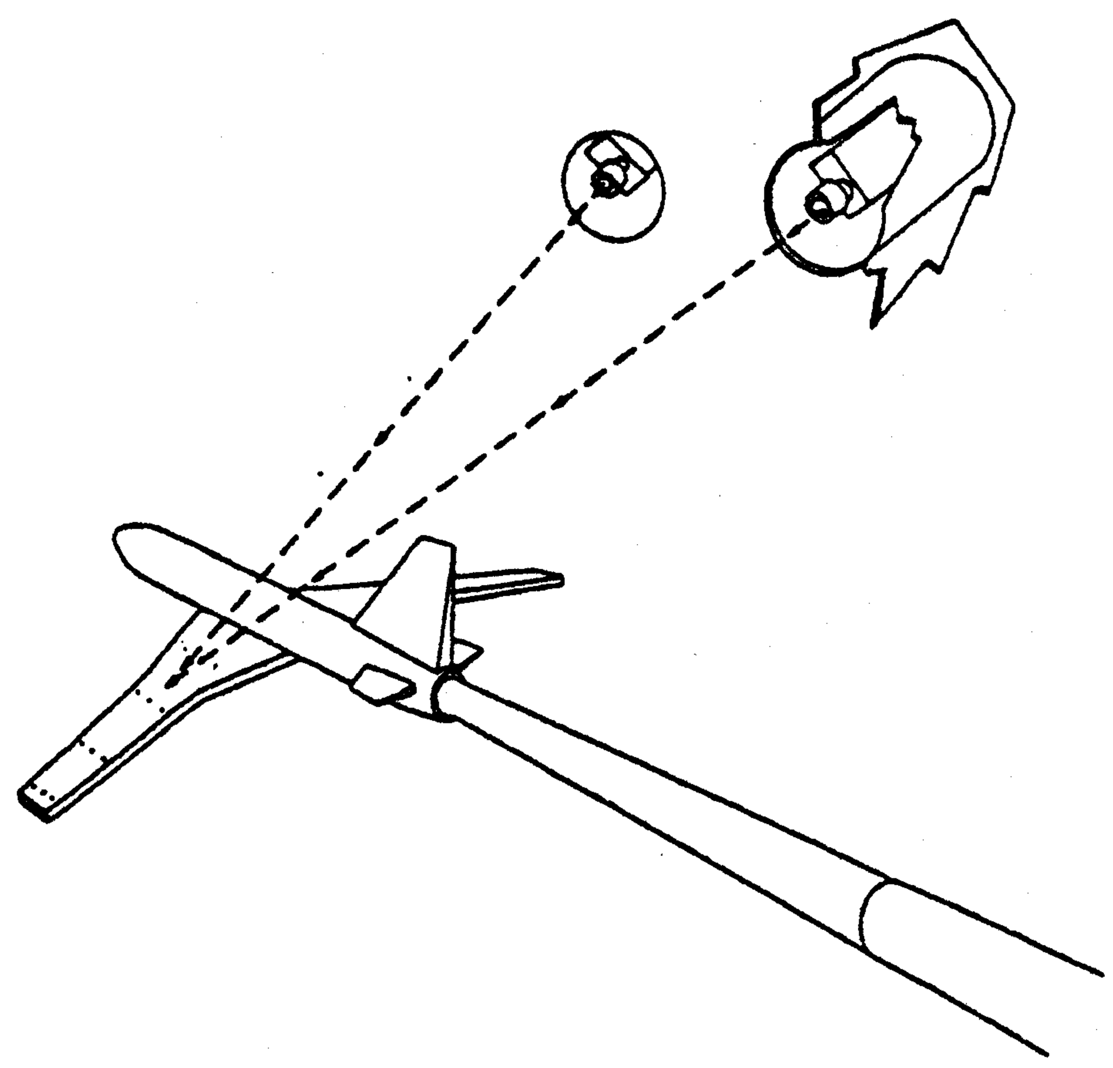

Fig. 1 Experimental configuration at the NTF

resolution (10 MHz) video disc records up to 150 video image pairs (one frame from each camera) when vibrations or model movement prevent use of the video hardcopy unit during a tunnel run. Permanent hardcopies are made of selected video images after the tunnel run is complete.

A calibration fixture consisting of 216 targets 1.3 mm in diameter on 2.5-cm-diameter aluminum rods located in two parallel planes was used as a test object (Figure 2).

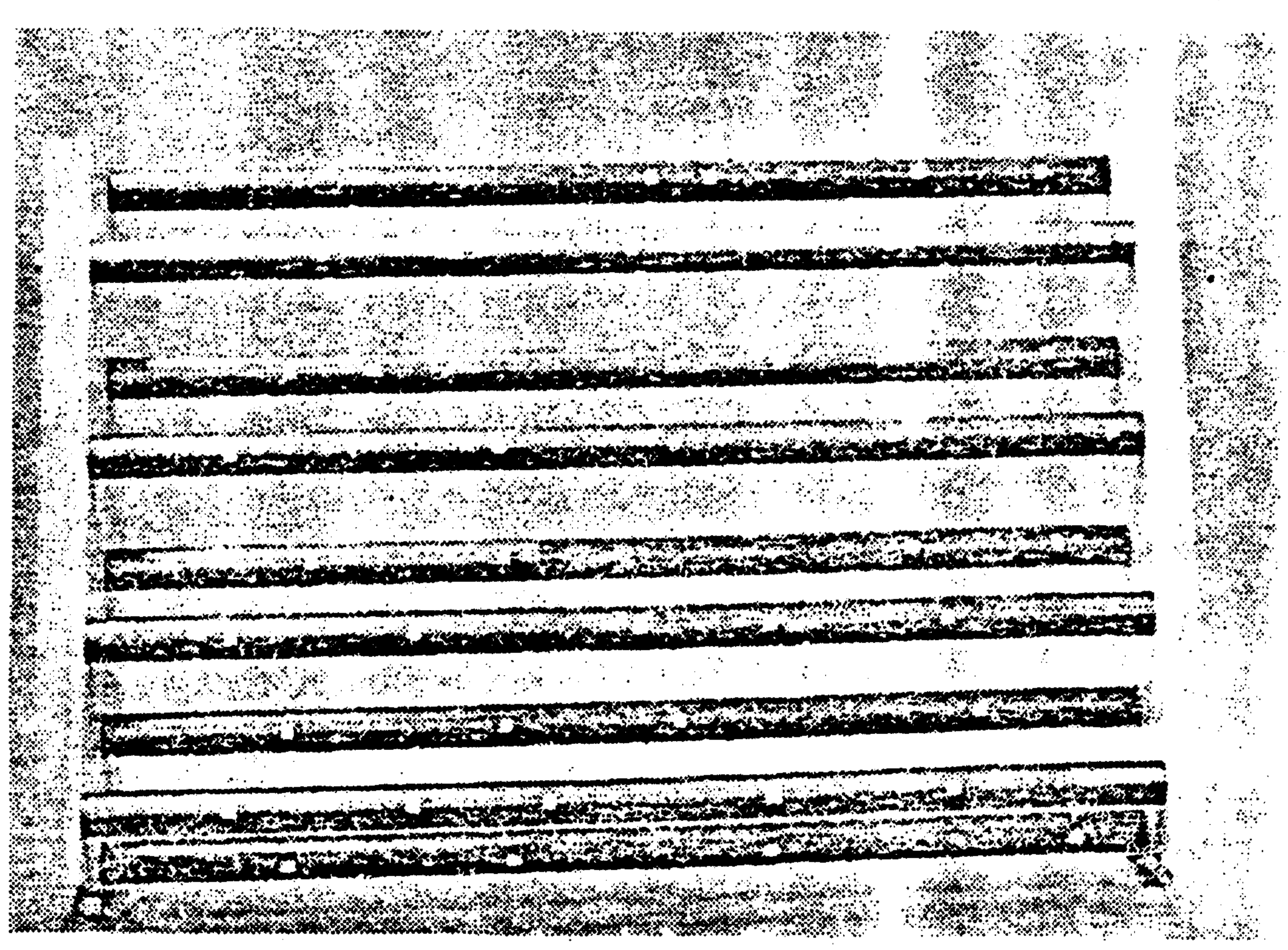

Fig. 2 Calibration fixture

The targets on the fixture cover a volume of approximately 7 x 40 x 60 cm. The targets were measured with a three axes coordinate measurement machine which had a resolution of 2.5 micrometers. Forty of the targets had been measured with a similar coordinate measurement machine 3 years earlier by a different operator. Since discrepancies in the measurements of these 40 targets were less than 0.05 mm rms, the calibration fixture was deemed a stable test object for these studies.

Data Reduction Without Distortion Correction

The Direct Linear Transformation (DLT) method (Abdel-Aziz and Karara 1971) was used for data reduction of video images uncorrected for distortion. In the DLT method the well known collinearity equations are rewritten as linear functions of 11 parameters.

$$x = \frac{L_1X + L_2Y + L_3Z + L_4}{L_9X + L_{10}Y + L_{11}Z + 1} \tag{1}$$

$$y = \frac{L_5X + L_6Y + L_7Z + L_8}{L_9X + L_{10}Y + L_{11}Z + 1} \tag{2}$$

The 11 parameters are then found by linear least squares if the location in object space of the corresponding image points from two cameras are known. The DLT method requires no initial estimates as do the collinearity equations and the replacement of a single camera constant with different constants in the x and y directions is inherent in the method. This allowance is necessary since video images may experience large differences in scale between the horizontal and vertical axes (Wong 1970). Once the DLT parameters are known, triangulations for unknown targets are performed by first rewriting equations (1) and (2) as linear functions of X, Y, Z so that linear least squares can be used to solve the four image equations (assuming two cameras) in three unknowns.

The DLT method was used for data reduction in earlier work at Langley with film cameras (Brooks and Beamish 1977). The use of the DLT method in our initial work with video cameras before distortion correction routines were established, gave much better results than the collinearity equations which did not allow for scale differences. If allowance is made for scale differences in the two axes then the DLT and collinearity equations give similar results. The desirability of using the collinearity equations for data reduction once the video images are corrected for distortion is discussed later.

Results Without Distortion Corrections

The results of photogrammetric measurements made with video images uncorrected for distortion (except for scale differences between axes) are presented in table 1. The coordinate system used in table 1 is that commonly used for wind tunnels--a right handed coordinate system in which X is in the direction of flow, Z is up and Y is along the wing span. The known target locations of the calibration fixture were used first to determine the DLT parameters. Images of points on the calibration fixture common to both cameras were then used for triangulation. The rms of the residuals from the known locations were then computed and are presented in table 1. For comparison photogrammetric measurements were also made with two Hasselblad 500 EL/M film cameras which used 80 mm focal length lenses. The formats of the film cameras were only about 1/3 filled.

Little difference was noted between data recorded on the hardcopy at 525 and 875 scan lines, although the appearance

Test	rms residuals, mm		
	X	Y	Z
Video/875/film	1.0	2.0	1.7
Video/875/hardcopy	0.4	0.7	0.6
Video/525/hardcopy	0.4	0.7	0.6
Film	0.2	0.5	0.2

Table 1 Results of photogrammetric measurements made with images uncorrected for distortion (except for scale differences between axes)

of the video images, especially under magnification of the comparator, was better for 875 scan lines. High resolution, while generally a desirable attribute, is not an absolute requirement for photogrammetry since the centroid of an image representing an unknown target location must be determined rather than the separation and resolving of two closely spaced images as is normally implied in the meaning of resolution. Since much of the support instrumentation available for video systems such as tape recorders, hardcopy devices, frame grabbers, etc. are designed for the more standard 525 raster scan rate, consideration is presently being given to operation of the NTF video cameras at 525 scan lines.

A substantial improvement was found by use of the dry silver video hardcopy device instead of a hand-held camera which uses 7.5 x 10 cm format positive/negative instant film to photograph the television display screen. This improvement was due to the large amount of distortion additionally suffered by photographing the curved video display screen. The negatives from the hand-held camera were easier to read on the monocomparator and had better readup repeatability ($\approx$ 0.006 mm) than the dry silver hardcopies ($\approx$ 0.013 mm), but if allowance is made for the larger scale of the images on the hardcopies (2.3 x hand-held camera) then the readup repeatabilities are comparable.

DISTORTION CORRECTIONS

In earlier work with video cameras for space applications (Wong 1970) it was established that geometrical distortions of video images were largely systematic and stable over long periods of time so that corrections for these distortions were possible. The nature of these distortions are discussed in the early references and are not reviewed here. The geometric distortions of video images consist of both electronic and optical distortions. The electronic distortions are unique to video images whereas the optical distortions are due to the imaging lens and are the same as in film camera photogrammetry. If the electronic distortions can be removed first, optical distortions can then be corrected as for film cameras.

Even though the electronic distortions are highly systematic and stable there may still be small variations of distortion with time which can only be accounted for with a reseau grid on the video tube. The reseau grids serve as fiducials to aline successive video images and to reference the location of the photogrammetric principal point. The reseau also aids in determinations of proper scale on the video tube face.

Both Vidicon and Newvicon tubes were purchased which had reseau grids consisting of a 7 x 9 array of equally spaced crosses with a nominal spacing of 1.35 mm. The reseau grids on the tubes were measured with a monocomparator. The tubes were mounted vertically, with the face of the tube up, on the traversing stage of the monocomparator. A separate microscope and illuminator were then used to sight on the reseau crosses. The tube and microscope were alined perpendicularly to the comparator traversing stage to within 0.5° with a bubble level. This alinement reduced cosine errors in the measurement to less than 0.5 micrometer over 10 mm. To check for possible movement of the tube during the readings of the 63 reseau crosses and to determine readup repeatability, the reseau grids were measured three times and mean and rms deviation from the mean computed for each reseau cross. The mean and standard deviations of both the horizontal and vertical spacings of the reseau grids were computed and found to be 1.347 and 1.346 mm with standard deviations of less than 0.002 mm in both directions.

<u>Long Term Stability of Electronic Distortion</u>

The mapping transformations involved in photogrammetry are commonly treated as polynomial expansions of the form

$$f(x,y) = c_1 + c_2x + c_3y + c_4xy + c_5x^2 + c_6y^2 + \ldots$$

Empirically, the following approximations were found useful in tracking the electronic distortion in the cameras

$$x' = a_1 + a_2x + a_3y + a_5x^2 \tag{3}$$

$$y' = b_1 + b_2x + b_3y + b_6y^2 \tag{4}$$

With this transformation, the video distortion patterns of two video cameras recorded on the video hardcopy unit are similar as shown in figure 3. If conformal transformation ($b_2 = -a_3$, $b_3 = a_2$; $a_n, b_n = 0$ for $n > 3$) is used instead, the differences in scale ratio between the x and y axes of the two video cameras tends to mask any similarity in the distortion patterns.

The distortion patterns have been noted to be relatively stable over periods of time of up to 3 months. In figure 4 data from nine video images recorded on dry silver paper over a period of 93 days are presented.

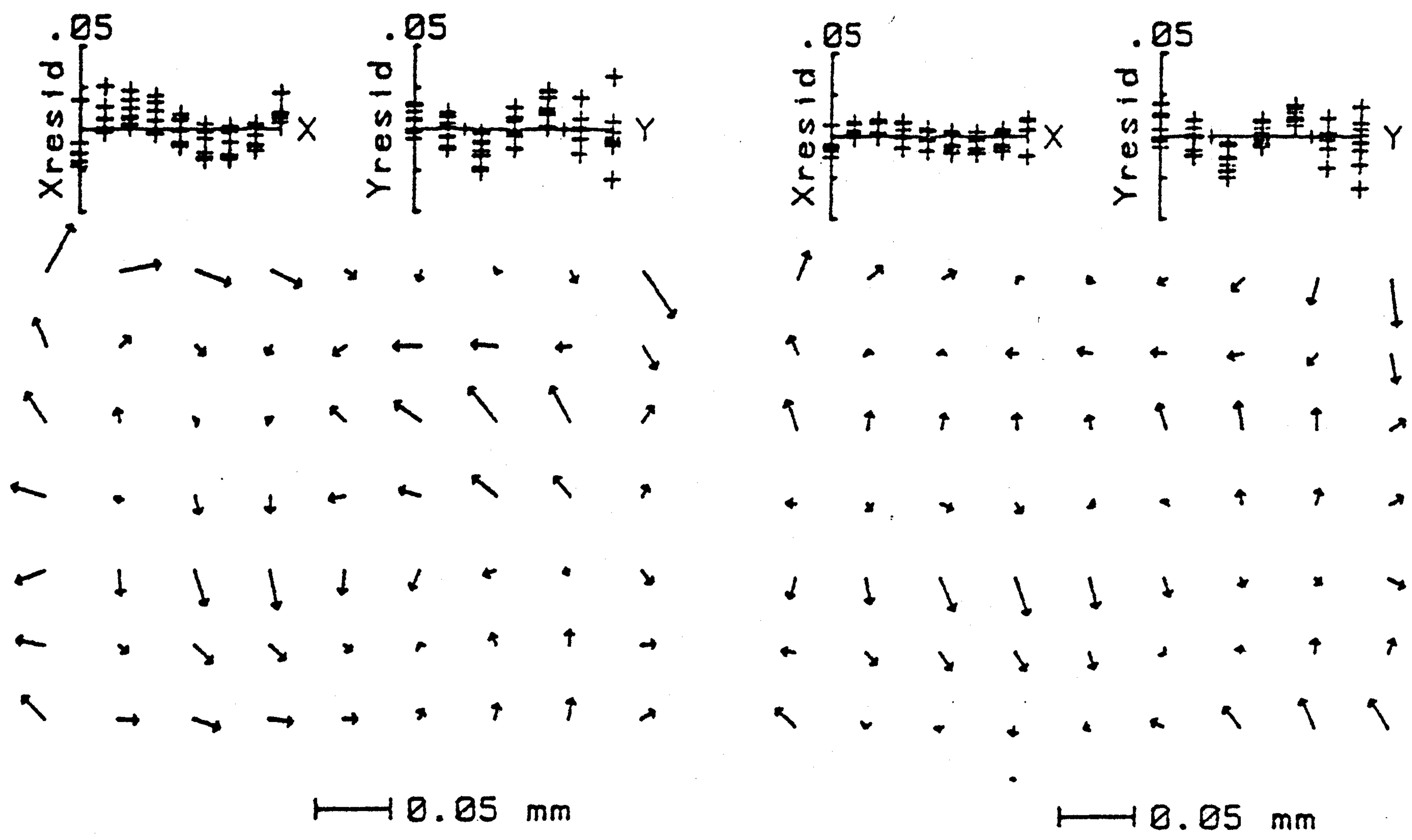

Figure 3. Electronic distortion patterns from two video cameras

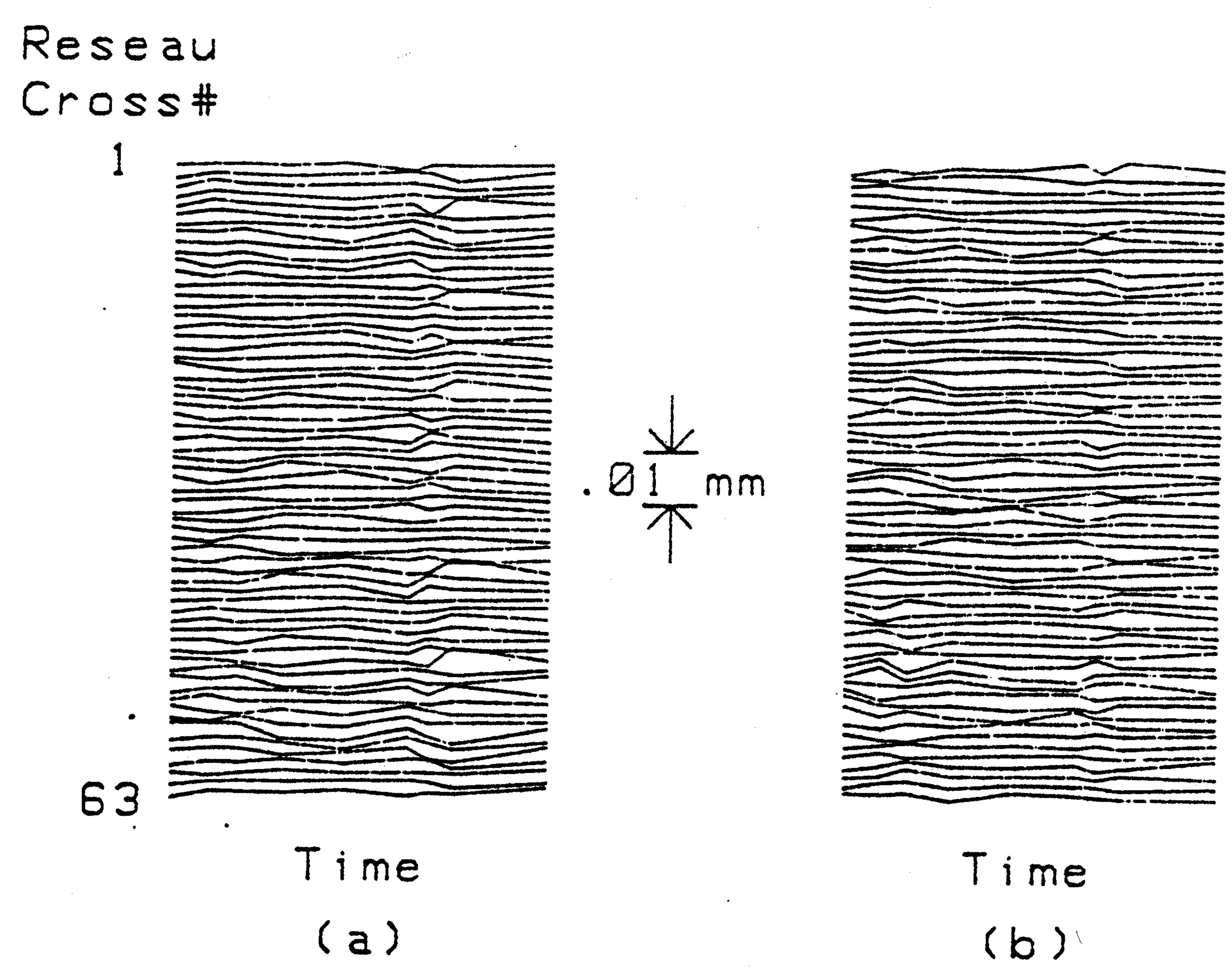

Figure 4. Electronic distortion variations over 93 days (a) X distortion (b) Y distortion

The vertical scale for those plots consists of the x and y distortion values at each of the 63 reseau crosses minus the mean of the distortion values of the 9 images so that relative changes in the distortion as a function of time are presented. The rms values of the difference from the mean for the 9 video images were computed for the 63 reseau crosses. The mean of the 63 rms values were then computed and found to be 0.0018 mm in the x and 0.0016 mm in the y directions. For 4 video images recorded within 1 hour the means of the 63 rms values in the x and y directions were 0.0017 mm which represents the short term distortion repeatability. For three readings of a single hardcopy recording of a video image the means in the x and y directions were 0.0006 mm which is an indication of the reading repeatability.

The x, y distortion residuals for each reseau cross as well as the transformation coefficients necessary to transform the video image to the video tube reseau grid are saved as a distortion correction data file for that particular video image. The distortion vectors are plotted and compared to previous distortion plots to check for the long-term changes in the distortion pattern or possible reading errors (blunders).

It is obvious from figure 3 that some systematic electronic distortion remains after this initial transformation. When all of the reseau crosses are visible on the video image (variations in lighting on the object may obscure some reseau crosses), bilinear interpolation is used to complete the electronic image refinement.

Bilinear Interpolation

With bilinear interpolation the distortion values of the four nearest reseaus are used to interpolate for the corrections to be applied to a given image point. Thus the image plane can be divided into a number of smaller frames with corners defined by four reseau crosses within which bilinear interpolation is used. For this reason Wong has called this method the Sub-Frame approach. The bilinear interpolation equations may be expressed as

$$\Delta x' = a_1 + a_2x' + a_3y' + a_4x'y' \qquad (5)$$

$$\Delta y' = b_1 + b_2x' + b_3y' + b_4x'y' \qquad (6)$$

where x' and y' are the coordinates after transforming with equations (3) and (4) and $\Delta x'$ and $\Delta y'$ are the corrections to be applied to the transformed image data to complete the electronic distortion refinement.

For each of the four nearest reseau crosses which surround an uncorrected image point a pair of such equations can be written. The a and b coefficients can then be found by solving the four equations in four unknowns. The equations (5) and (6) are linear for constant x' or y' and quadratic for an image line which is not parallel to the x' or y' axes.

Bilinear interpolation is begun for a transformed image point by first determining which four reseau crosses are its nearest neighbors. The finding of the four nearest neighbors can be the most time consuming part of the electronic distortion correction procedure. The procedure employed is to first treat the reseau crosses as being undistorted to arrive at initial values for the four nearest neighbors. The actual distorted location of these four reseau crosses are then used to construct a quadrilateral to verify that the uncorrected image point lies within. If not, two of the old values of nearest neighbors are replaced with the appropriate two new values and the quadrilateral test repeated. Once it is verified that the uncorrected image point lies within the quadrilateral formed by four reseau crosses, equations (5) and (6) are solved using the known distortion values of the four reseau crosses. The distortion corrections are then applied to the transformed image point. This procedure is repeated until all image points have been corrected for electronic distortion or flagged as being outside the reseau grid and hence uncorrected since extrapolation is not allowed.

If all the reseau crosses are not visible distortion corrections can still be made if a distortion correction data file from a previous video image in which all the reseau crosses are visible is used. The transformation equations (3) and (4) are used to fit the current video image to the video image corresponding to the distortion correction data file (reference video image) in the least squares sense. After the transformation of the current video image to the reference video image the transformation to the video tube reseau grid can then be applied. The correction procedure for the uncorrected image points then proceeds as above.

High-Order Polynomial Interpolation

To characterize the distortion of video images Wong has developed the following set of polynomials (Wong 1973)

$$\begin{aligned}\Delta x = {} & a_1 + a_2 x + a_3 y + a_4 xy + a_5 x^2 + a_6 y^2 + a_7 x^2 y \\ & + a_8 xy^2 + a_9 x^3 + a_{10} y^3 + a_{11} x^3 y + a_{12} xy^3 \\ & + a_{13} x^4 + a_{14} y^4 + a_{15} x^2 y^2 + a_{16} x^3 y^2 \\ & + a_{17} x^2 y^3 + a_{18} x^5 + a_{19} y^5 + a_{20} x^3 y^3\end{aligned} \tag{7}$$

$$\Delta y = b_1 + b_2 x + b_3 y + b_4 xy + \ldots + b_{20} x^3 y^3 \tag{8}$$

This 20 coefficient set is an extension of a lower order set of polynomials (14 coefficients each) which he developed theoretically to account for various sources of distortion in video images. In the high-order polynomial interpolation approach all the reseau cross distortion data are used at one time, first for the x and then for the y terms, in a linear least squares reduction to determine the 20 coefficients each for the x and y distortion corrections. Since all the reseau crosses are used at one time Wong refers to this method as the full-frame polynomial method. He obtained excellent experimental results when correcting video images with this method. Wong did not have an auxiliary calibrated grid in his video images to verify the bilinear interpolation method and so did not test that approach.

Once the 20 coefficients each for the x and y directions are found the video image points can then be corrected to give a video image which is scaled and alined with the reseau grid on the video tube (just as for bilinear interpolation. Not all the 20 coefficients for the x and y directions are significant as noted by comparing the standard deviations of the coefficients to the coefficients themselves. The insignificant coefficients can be deleted and a reduced number of coefficients solved for if desired. Just as for bilinear interpolation, if all the reseau crosses are not available the current video image can be transformed by least squares using equations (3) and (4) to a reference video image for which the high order polynomial coefficients are known. Then the polynomial coefficients for the reference video image can be used to correct the current video image for electronic distortions.

Verification of Electronic Distortion Correction Methods

In order to verify the corrections for electronic distortion a reticle was placed in contact with the faceplate of a video tube (with lens removed) which was illuminated by collimated light derived from a zirconium arc lamp placed at the focus of a well-corrected telescope doublet. The reticle consisted of a line with 43 tic marks which had been measured with a monocomparator to 0.003 mm. The corrected image plane coordinates of the video image could then be fitted by nonlinear least squares using a 2-D conformal transformation with scale fixed at unity to the known values of the reticle to determine the residuals before and after correcting for electronic distortion. The 63 reseau crosses and the reticle as positioned for one test are depicted in figure 5.

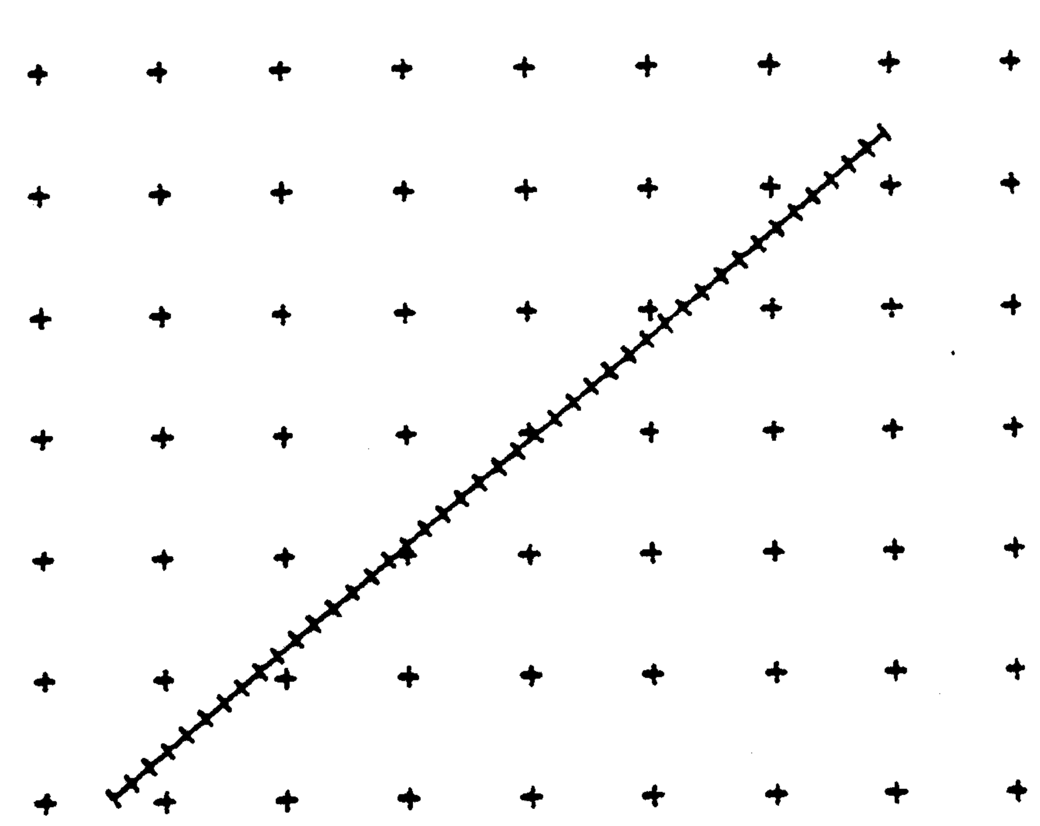

Fig. 5 Reticle location on tube

The uncorrected distortion vectors after least squares conformal transformation to the tube face reseau grid are shown in figure 6. The residuals after correcting for electronic distortion using both bilinear and high-order polynomial interpolation are also shown in figure 6.

The rms values of the uncorrected distortion vectors were 0.008 mm and 0.012 mm in the x and y directions. After correction the rms residuals were reduced to 0.0031 and 0.0032 mm using bilinear interpolation and 0.0032 and 0.0034 mm using high-order polynomials. Plots of the x and y residuals before and after correction by the two techniques are shown in figure 7. The video image hardcopy recording for these tests was read three times on a monocomparator. The repeatability after transforming to

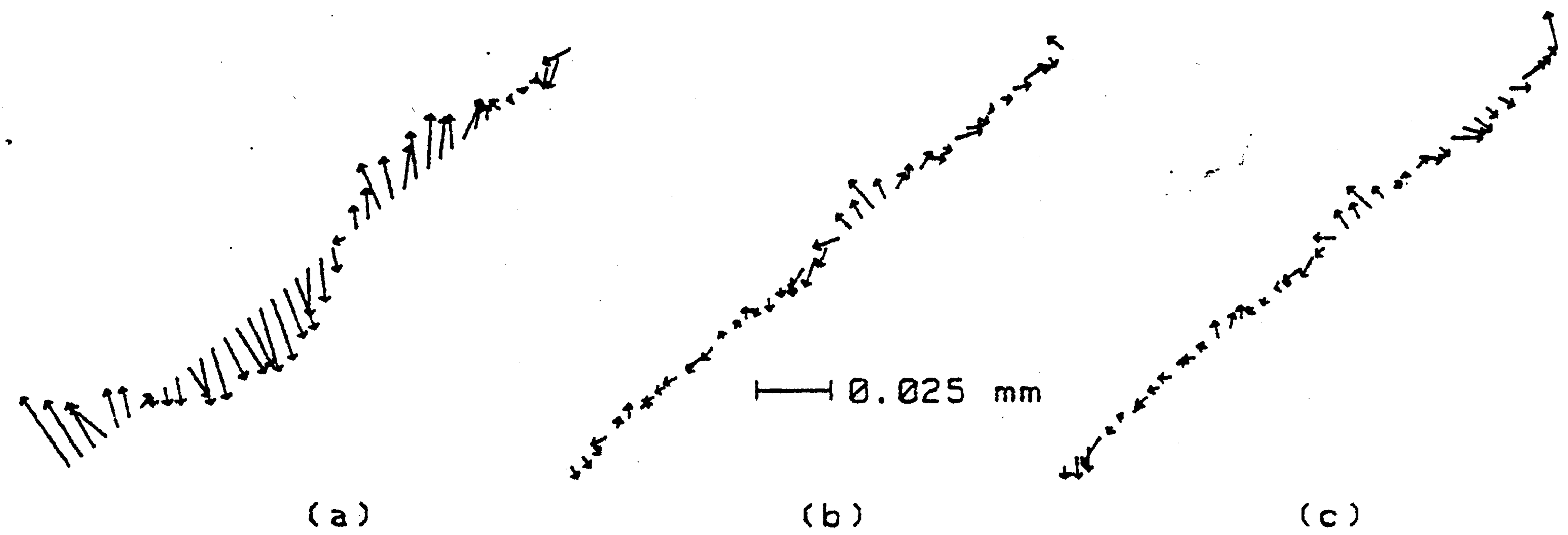

Figure 6. Distortion vectors (a) uncorrected and after correction with (b) bilinear interpolation and (c) high-order polynomial interpolation

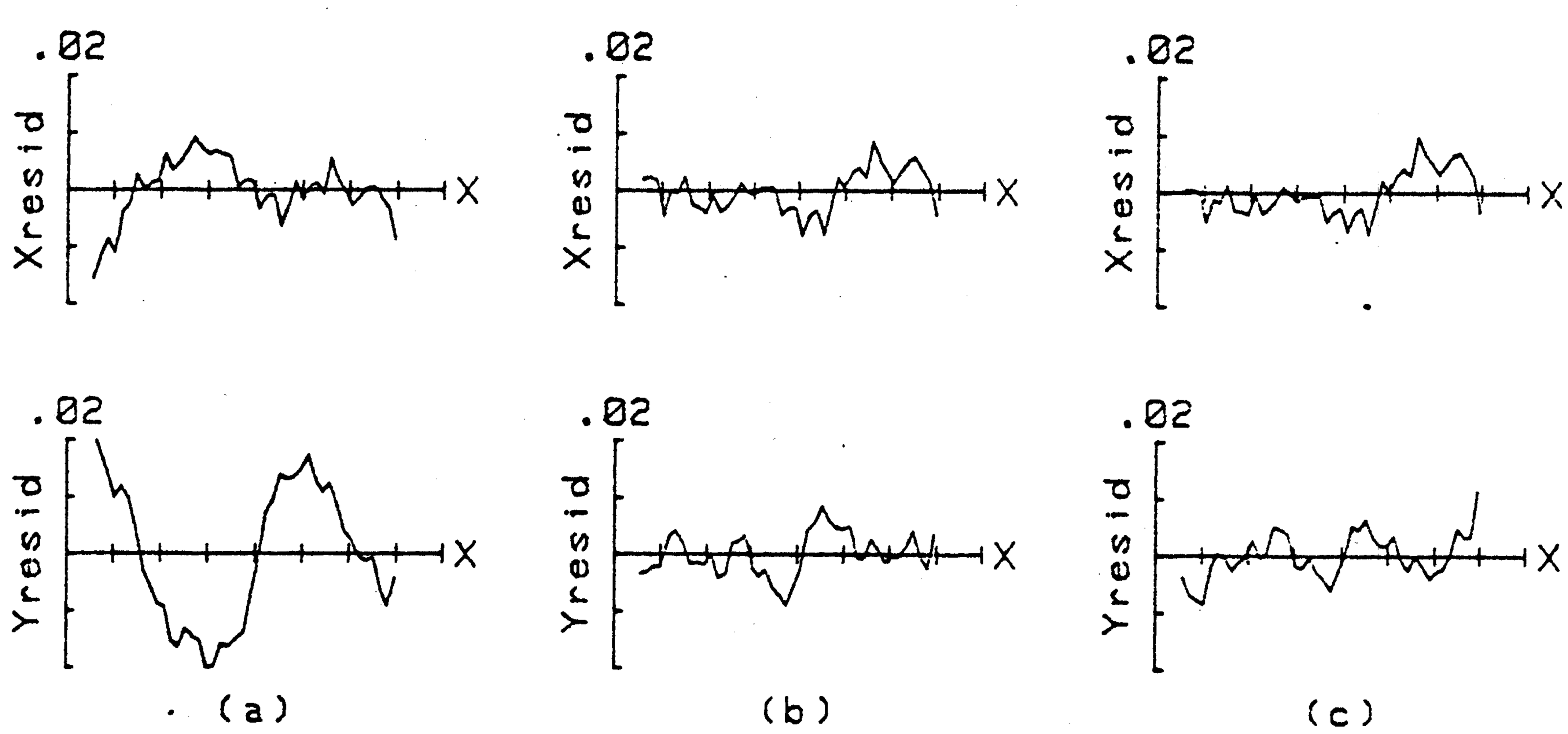

Figure 7. Distortion residuals (a) uncorrected and after correction with (b) bilinear interpolation and (c) high-order polynomial interpolation

the tube reseau grid was 0.0007 mm in x and y. The repeatability of reading the tic marks was 0.0014 mm in x and y after transforming to the tube reseau grid.

As a further comparison both bilinear and high-order polynomial interpolation were used to correct points along a line in the y direction for the above video image. Figure 8 portrays the x and y distortion corrections versus y for both types of interpolations. Superimposed on the plots are the distortion values at the seven reseau crosses which are nearly passed through by a vertical line with x = 0. While both methods give acceptable results the oscillatory nature of high-order polynomial interpolation may tend to under or over estimate the distortion

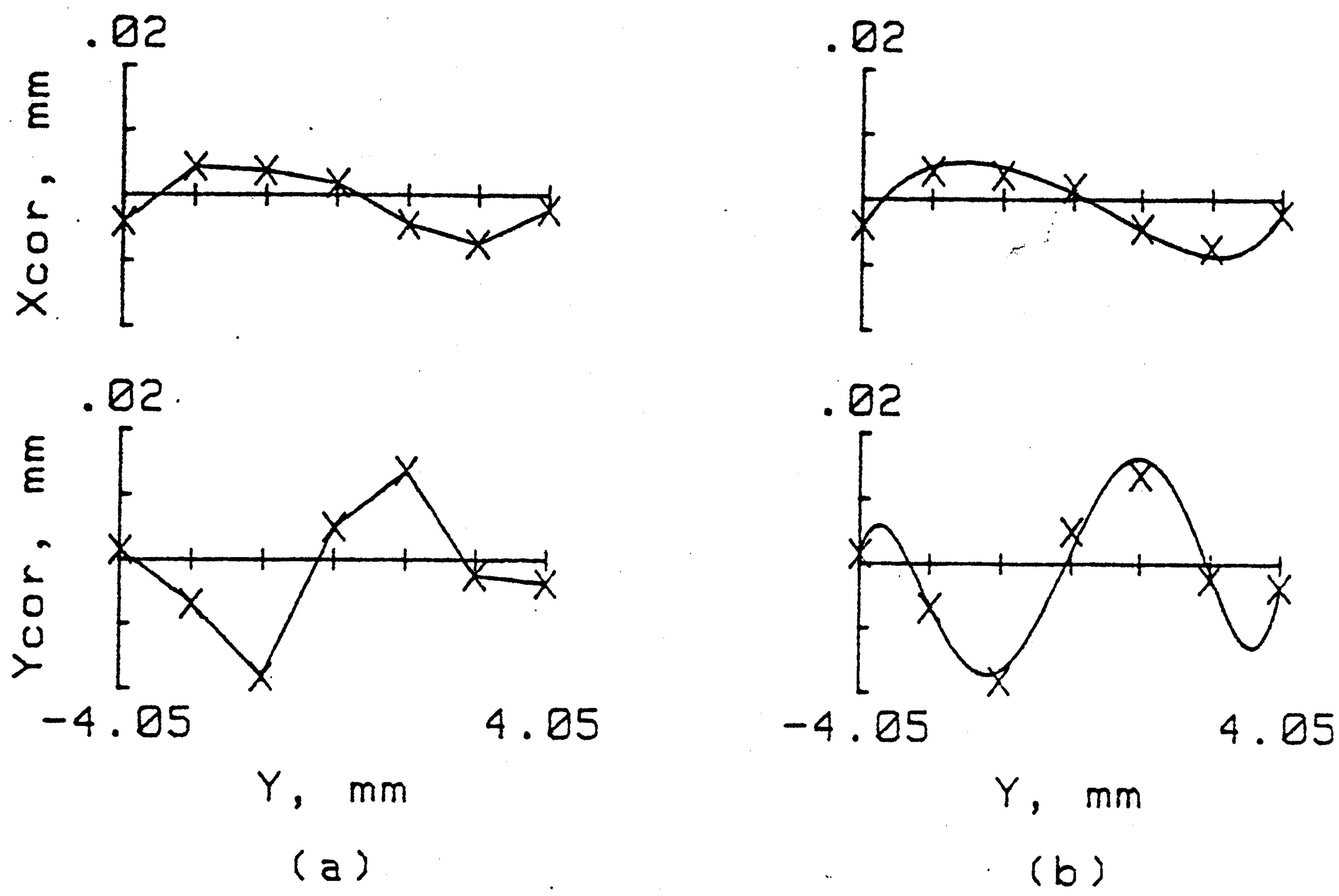

Figure 8. Comparison of (a) bilinear and (b) high-order polynomial interpolation

correction necessary in some regions of the video image. Given accurately measured reseau marks there is no strong justification for using other than bilinear interpolation between points.

Corrections for Lens Distortion

Once corrections for electronic distortion have been applied it is possible to correct for optical lens distortion by the plumb line method (Brown 1972). Several standard television lenses were found to suffer primarily from barrel distortion which is adequately modeled by a single third order radial distortion coefficient σ.

The desired coordinates x_c and y_c corrected for lens distortion can be expressed in terms of the measured coordinates x and y (which are corrected for electronic distortion only) as

$$x_c = x - \sigma r_c^2 (x_c - x_p) \approx x - \sigma r^2 (x - x_p) \tag{9}$$

$$y_c = y - \sigma r_c^2 (y_c - y_p) \approx y - \sigma r^2 (y - y_p) \tag{10}$$

where $r_c = \left[(x_c - x_p)^2 + (y_c - y_p)^2\right]^{1/2}$, $r = \left[(x - x_p)^2 + (y - y_p)^2\right]^{1/2}$, and x_p and y_p locate the photogrammetric principal point. The approximations in equations (9) and (10) are justified since the distortion computed using

x, y is very nearly the same as when using x_c, y_c.

The equations which describe the corrected (for electronic and lens distortion) image location of a number of vertical parallel straight lines are of the form

$$x_c - my_c - b_x = 0 \tag{11}$$

where m is the slope of the lines and b_x is the x axis intercept which differs for each line. Equation (11) can be rewritten using equations (9) and (10) and taking $x_p = y_p = 0$ as

$$x - \sigma r^2 x - my + m\sigma r^2 y - b_x = 0 \tag{12}$$

There will be one such equation for each parallel line. These equations (one for each image point of each line) can then be solved with nonlinear least squares to yield common values for σ and m and separate values of b_x, the x intercept, for each parallel line. Figure 9 depicts the results of such an analysis for a standard 50 mm focal length television lens.

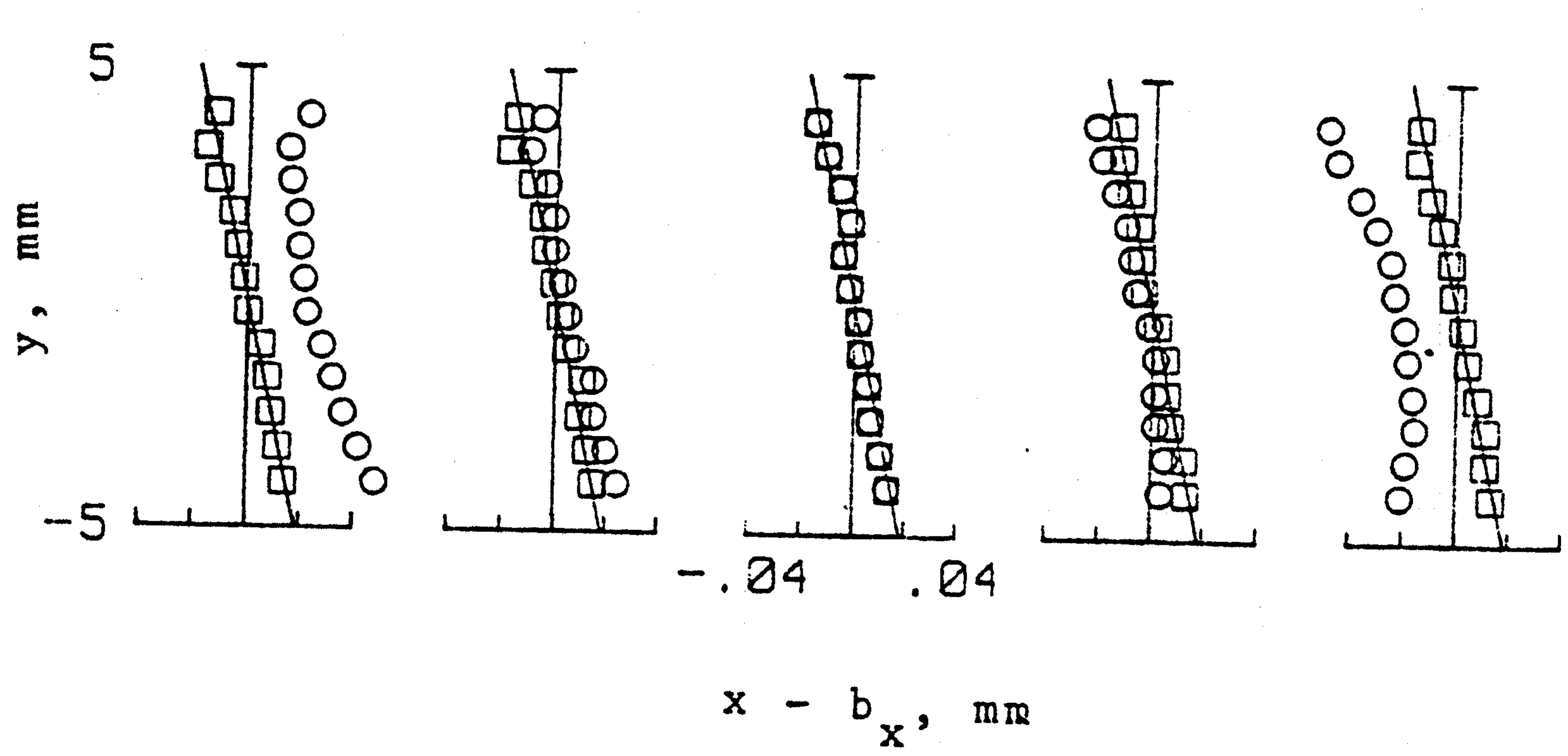

Figure 9. Distortion of a standard television lens

For these tests five plumb lines were hung in a plane 2 meters from the camera. The camera was tilted slightly which accounts for the slope in the data. The circles represent image data corrected for electronic distortion but uncorrected for lens distortion. The solid lines are plotted using the least squares estimates of the slope and x intercepts. The squares represent the measured image data after correcting for lens distortion with the least squares estimate for σ. The least squares estimate for σ was -1.5×10^{-4} mm^{-2} with a standard deviation of 1×10^{-5} mm^{-2}. The rms value of the residuals after the least squares reduction was 1.7 micrometers. Very little variation in σ with object distance was noted for a fixed lens focus setting. A least squares reduction expanded to include 5th order radial distortion in addition to third order did not reduce the residuals significantly.

If in the least squares reductions for radial lens distortion x_p and y_p are not set to 0 and are taken instead as two additional coefficients to be solved for, then the least squares estimates for σ change less than 1 standard deviation from the reductions in which x_p and y_p are taken to be 0. Thus the least squares reduction for σ is only weakly dependent on x_p and y_p as pointed out by Brown 1972. In addition the least squares extimates for x_p and y_p are generally one to two times larger than the standard deviations of their estimates. Thus it is justifiable to take x_p and $y_p = 0$ in determinations of the radial lens distortion coefficient σ.

PHOTOGRAMMETRIC MEASUREMENTS AFTER APPLYING DISTORTION CORRECTIONS

The video image data, after correcting for both electronic and lens distortions, can be treated as if from a film camera and reduced with the collinearity equations (Manual of Photogrammetry 1980).

$$x - x_p + \frac{c[m_{11}(X - X^c) + m_{12}(Y - Y^c) + m_{13}(Z - Z^c)]}{m_{31}(X - X^c) + m_{32}(Y - Y^c) + m_{33}(Z - Z^c)} = 0 \quad (13)$$

$$y - y_p + \frac{c[m_{21}(X - X^c) + m_{22}(Y - Y^c) + m_{23}(Z - Z^c)]}{m_{31}(X - X^c) + m_{32}(Y - Y^c) + m_{33}(Z - Z^o)} = 0 \quad (14)$$

x and y are the corrected video image data (x_c, y_c in previous notation). The m's are elements of the rotation matrix and are functions of ω, ϕ, k--the rotation angles of the camera. X, Y, Z are the coordinates in object space corresponding to the image. X^c, Y^c, Z^c locate the camera perspective center.

If the camera constant c and the location of the photogrammetric principal point x_p, y_p are known then the unknowns in the collinearity equations are reduced by three. The collinearity equations can then be used for space resection to determine the six elements of exterior orientation--ω, ϕ, k, X^c, Y^c, Z^c--of each camera for image data which lies on a plane. This is not possible with the DLT method or the collinearity equations when c, x_p, and y_p are carried in the reduction as additional unknowns. The use of nearly planar image data to determine the exterior orientation of cameras occurs at the NTF when checking for possible changes in the cameras' precalibrated exterior orientation. These positional or angular changes may occur due to tunnel contraction when cold. Either known target points on the model or known targets on a test section wall which are in the background of the video images may be used to check and possibly adjust the precalibrated exterior orientations of the cameras.

A similar method to that recommended by Brown (1972) was used to determine c, x_p, and y_p. Four video images from a single camera at three positions were made of the calibration fixture. These video images were corrected for electronic and lens distortion (with the approximation $x_p = y_p = 0$). At one position the video camera was rolled 90° for one of the views as recommended by Brown. The collinearity equations were then used in a nonlinear least squares reduction to determine estimates of the four sets of exterior orientations and the common values of c, x_p, and y_p. c was found to be 50.93 mm with a standard deviation of 0.15 mm. x_p and y_p were found to be -0.15 and -0.10 mm with standard deviations of 0.08 and 0.11 mm. Due to the large value of the standard deviations of x_p and y_p in relation to their least squares estimates, x_p and y_p are taken to be 0 for photogrammetric measurements made at the NTF.

To judge the relative decrease in uncertainty due to the application of electronic lens distortion corrections, two video images of the calibration fixture were recorded. The video hardcopies were read on a monocomparator and reduced without any corrections using the DLT method. The collinearity equations with $x_p = y_p = 0$ and $c = 51.0$ mm were used to reduce the data with electronic corrections only and with both electronic and lens corrections. A summary of the results is presented in table 2. The rms residuals in

Correction	rms residuals, mm		
	X	Y	Z
None	0.3	0.8	0.5
Electronic	0.2	0.6	0.4
Electronic + lens	0.1	0.3	0.2

Table 2. Results of photogrammetric measurements made with video images with various levels of distortion correction applied

table 2 are computed by comparing the known locations of the calibration fixture to the values computed from triangulating on points common to both video images.

CONCLUDING REMARKS

Close-range photogrammetry with video cameras uncorrected for electronic or optical distortion is useful if allowance is made for scale change between the two axes. A convenient computational method for uncorrected video images is the Direct Linear Transformation. Electronic distortion correction can further reduce the uncertainty. Either bilinear or high order polynomial interpolation are suitable correction methods. Once electronic corrections have been made, optical lens distortion corrections can then be made. A simple correction for third order radial distortion is sufficient to remove most of the lens distortion. Once electronic and lens distortion corrections have been applied the collinearity equations can be used for data reduction. Fixing x_p and $y_p = 0$ and knowing c, it is possible to resect on planar data, which is an advantage in wind tunnel applications. Work is currently underway at the NTF to solve several operational problems caused by vibrations and low temperature operation. The results of this work as well as efforts to verify the accuracy of the video photogrammetry system will be reported later.

REFERENCES

Abdel-Aziz, Y. F. and Karara, N. M. 1971, Direct Linear Transformation From Comparator Coordinates Into Object Space Coordinates in Close-Range Photogrammetry. Close Range Photography Symposium, Urbana, Ill.

Brooks, J. D. and Beamish, J. K. 1977, Measurement of Model Aeroelastic Deformations in the Wind Tunnel at Transonic Speeds Using Stereo-photogrammetry. NASA TP 1010.

Brown, D. C. 1972, Calibration of Close Range Cameras. XII Congress of the International Society of Photogrammetry.

Burner, A. W., Snow, W. L., and Goad, W. K. 1983, Video Model Deformation System for the National Transonic Facility. NASA TM 85681.

Howell, R. R. 1980, The National Transonic Facility: Status and Operational Planning. A Collection of Technical Papers--AIAA 11th Aerodynamic Testing Conference, pp. 1-9.

Sieffert, J. A. 1982, CRT Image Distortion Determination Experiment. Rome Air Devel. Ctr. AF Syst. Command RADC-TR-82-239.

Slama, C. C. 1980, ed. Manual of Photogrammetry, Fourth ed. ASP, Falls Church, VA.

Wong, K. W. 1970, Fidelity of Space TV. Photo. Eng. Vol. 36, pp. 491-497.

Wong, K. W. 1973, Analysis of RBV Television System. Photo. Eng. Vol. 39, pp. 851-861.

Wong, K. W. 1975, Geometric and Cartographic Accuracy of ERTS-1 Imagery. Photo. Eng. and Remote Sensing Vol. 41, pp. 621-635.